Environ Earth Sci (2017) 76:492
DOI 10.1007/s12665-017-6827-y

ORIGINAL ARTICLE

Testing the potential of Sentinel-1A TOPS interferometry for the detection and monitoring of landslides at local scale (Veneto Region, Italy)

S. Fiaschi[1] · M. Mantovani[2] · S. Frigerio[2] · A. Pasuto[2] · M. Floris[1]

Received: 13 November 2016 / Accepted: 12 July 2017 / Published online: 19 July 2017

Abstract The recent Sentinel-1 mission, started by the European Space Agency in April 2014, provides the scientific community with new capabilities for the monitoring of the Earth surface. In particular, the Terrain Observation by Progressive Scans imaging technique used in the Interferometric Wide swath acquisition mode permits to acquire data over very wide areas (250 km of swath extension) at 20-m spatial resolution, with 12-day revisit time, making it suitable for ground displacement monitoring applications. With more than 1 year of synthetic aperture radar images available, it is now possible to carry out monitoring activities of slow moving phenomena such as landslides at both regional and local scales. In this work, the potential of Sentinel-1A for the monitoring of shallow (from 2 to 6 m of depth) landslides occurring in the North-Eastern Italian Pre-Alps was tested. Two stacks of Sentinel-1A scenes acquired in both ascending and descending orbits were processed using the Permanent Scatterer Interferometry (PSI) technique. The results, analysed in terms of PS density and quality, were compared with the ERS-1/2 and ENVISAT PSI database available from the Italian National Cartographic Portal to assess the capabilities of Sentinel-1A in detecting and monitoring landslides in respect to the previous satellite missions. The results of this work show the great potential of Sentinel-1A in the continuous monitoring of landslide-prone territories even at local scale. The achievable results can provide information that is useful to delineate the spatial and temporal evolution of landslides and precisely assess their rates of deformation.

Keywords Sentinel-1 · DInSAR · Landslide · Persistent scatterer · Time series

✉ S. Fiaschi
simone.fiaschi@phd.unipd.it

M. Mantovani
matteo.mantovani@irpi.cnr.it

S. Frigerio
simone.frigerio@irpi.cnr.it

A. Pasuto
alessandro.pasuto@irpi.cnr.it

M. Floris
mario.floris@unipd.it

[1] Department of Geosciences, University of Padova, Via G. Gradenigo 6, 35131 Padua, Italy

[2] CNR-IRPI: National Research Council of Italy - Research Institute for Geo-Hydrological Protection, Corso Stati Uniti 4, 35127 Padua, Italy

Introduction

In the last years, Advanced Differential Synthetic Aperture Radar Interferometry (A-DInSAR) techniques have been widely used to detect, monitor and characterize displacements triggered by natural processes such as subsidence (Tomás et al. 2014), earthquakes (Wright et al. 2006), deflation and inflation of volcanoes (Biggs et al. 2009) and slope movements (Wasowski and Bovenga 2014). In the case of landslides, the results obtained from A-DInSAR analyses are often not completely satisfying (Cascini et al. 2010). The reasons are to be found in both the technique and in the deformation process itself. On the one hand, the geometry of acquisition of the space-borne SAR sensors coupled with the topography of the area of interest causes shadowing effects and geometric distortions (i.e. foreshortening and overlay); on the other hand, the typology of the investigated landslide, in terms of slope, aspect, activity and the presence of vegetation, decorrelates the signal

between the acquisitions (Chaabane et al. 2005; Colesanti and Wasowsky 2006; Wasowski and Bovenga 2014; Wasowski et al. 2012). To tackle some of these limitations, the exploitation of data set acquired by missions with more suited wavelengths and shorter revisiting time has been proposed (Tosi et al. 2016; Wasowski and Bovenga 2014). Furthermore, to detect and monitor landslides occurring over vegetated areas or to measure large displacement rates and ignore phase decorrelation, other algorithms based on the amplitude offset tracking were developed (Casu et al. 2011; Manconi et al. 2014; Michel and Avouac 1999; Singleton et al. 2014).

The Sentinel-1A mission, operated by European Space Agency (ESA) since April 2014, provides the scientific community with improved capabilities for the quasi-continuous monitoring of the Earth surface. The Terrain Observation by Progressive Scans (TOPS) imaging technique, used in the Interferometric Wide swath (IW) acquisition mode, permits to generate SAR images over very wide areas (250 km swath dimension) at 20-m spatial resolution, with 12-day of revisiting time. Since April 2016, the launch of the twin satellite Sentinel-1B enhanced this temporal sampling capability by reducing the revisiting time to 6 days. With these increased interferometry-oriented design capabilities, the Sentinel-1 mission represents a very promising tool for ground displacement monitoring applications and at present, with almost 2 years of data acquisition, it is possible to carry out A-DInSAR analyses of landslides at both regional and local scales. Some authors have already successfully tested the potential of Sentinel-1A data in updating landslide inventory maps and monitoring landslide activity (Barra et al. 2016; Crosetto et al. 2016; Lazecky et al. 2016; Wasowski et al. 2016). Even if different methods to assess the a priori effectiveness of interferometric techniques have been proposed (Cascini et al. 2009; Colombo et al. 2006; Plank et al. 2012, 2013), additional tests in different geo-environmental scenarios are needed, because the quality of the results, in particular for landslide analyses purposes, depends on several factors related to the geo-environmental features of the area under investigation and to the processing technique (Hanssen 2005; Mahapatra et al. 2012), which can limit the reproducibility of the interferometric results in different areas (Wasowski and Bovenga 2014).

In this work, the potential of Sentinel-1A acquisitions to detect and monitor landslide phenomena affecting a densely vegetated area located in the North-Eastern Italian Pre-Alps is tested. More than 40 images acquired from ascending and descending orbits were processed using the Persistent Scatterer Interferometry (PSI) technique (Ferretti et al. 2001). The results were compared with the ERS-1/2 and ENVISAT PSI database available from the Italian National Cartographic Portal (http://www.pcn.minambiente.it). The quality of the outcomes was assessed in terms of persistent reflectors density and measurement accuracy (Colesanti and Wasowsky 2006) over the entire study area; in particular, the observations on two specific active slopes are reported and discussed. The strengths and weaknesses of the Sentinel-1A TOPS mode interferometry emerged during this study were likewise pointed out.

Study area

The Municipality of Trissino covers an area of about 22 km^2 in the Province of Vicenza (Veneto Region, Italian Pre-Alps, NE Italy) (Fig. 1). The Municipality of Trissino covers an area of about 22 km^2 in the Province of Vicenza (Veneto Region, Italian Pre-Alps, NE Italy) (Fig. 1). The territory is characterized by hillslope morphologies with elevations ranging from 800 m a.s.l. (West) to 100 m a.s.l. (South). The geology of the area (Fig. 1), typical of the eastern Lessini Mountains, is characterized by widespread Palaeocene, Middle Eocene and Oligocene volcanic activity and by the deposition of shallow water carbonates (McCann 2008). The Upper Palaeocene is characterized by the deposition of volcanic rocks (basalts, hyaloclastites and volcanoclastites) intercalated with marine carbonate deposits (Beccaro et al. 2001). The Lower Eocene sediments consist of thin and discontinuous marly limestones (Garavello and Ungaro 1996). High volumes of basaltic rocks originated during the volcanic activity of the Middle Eocene. In the Upper Eocene, marls and calcarenites started to deposit with increasing sedimentation rates until the Upper Oligocene. The volcanic formations are generally covered by Quaternary eluvial and colluvial deposits originated from the alteration of the bedrock.

The entire area is affected by a large number of different ground instabilities (Fig. 2), which have been detected and classified according to Cruden and Varnes (1996) combining the information provided by the Italian Landslide Inventory (IFFI) archive compiled in 2008 and the geomorphological map produced by the 2013 Italian Territory Development Plan (PAT) project. This information was updated through the analysis and interpretation of the available aerial photographs and orthophotos acquired from 1954 to 2010. A total of 64 landslides, affecting the 18% of the Municipality of Trissino, have been reported and classified by three main types of movement (Fig. 2): earth flow, roto/translational slide and complex. Such instabilities are generally triggered by intense rain events as occurred in November 2010, when an exceptional event (up to 500 mm of cumulated rainfall in 3 days) hit the Vicenza Province and the entire NE Italy causing several floods and triggering a very large number of mass movements. During the floods, the Soil Protection Division of

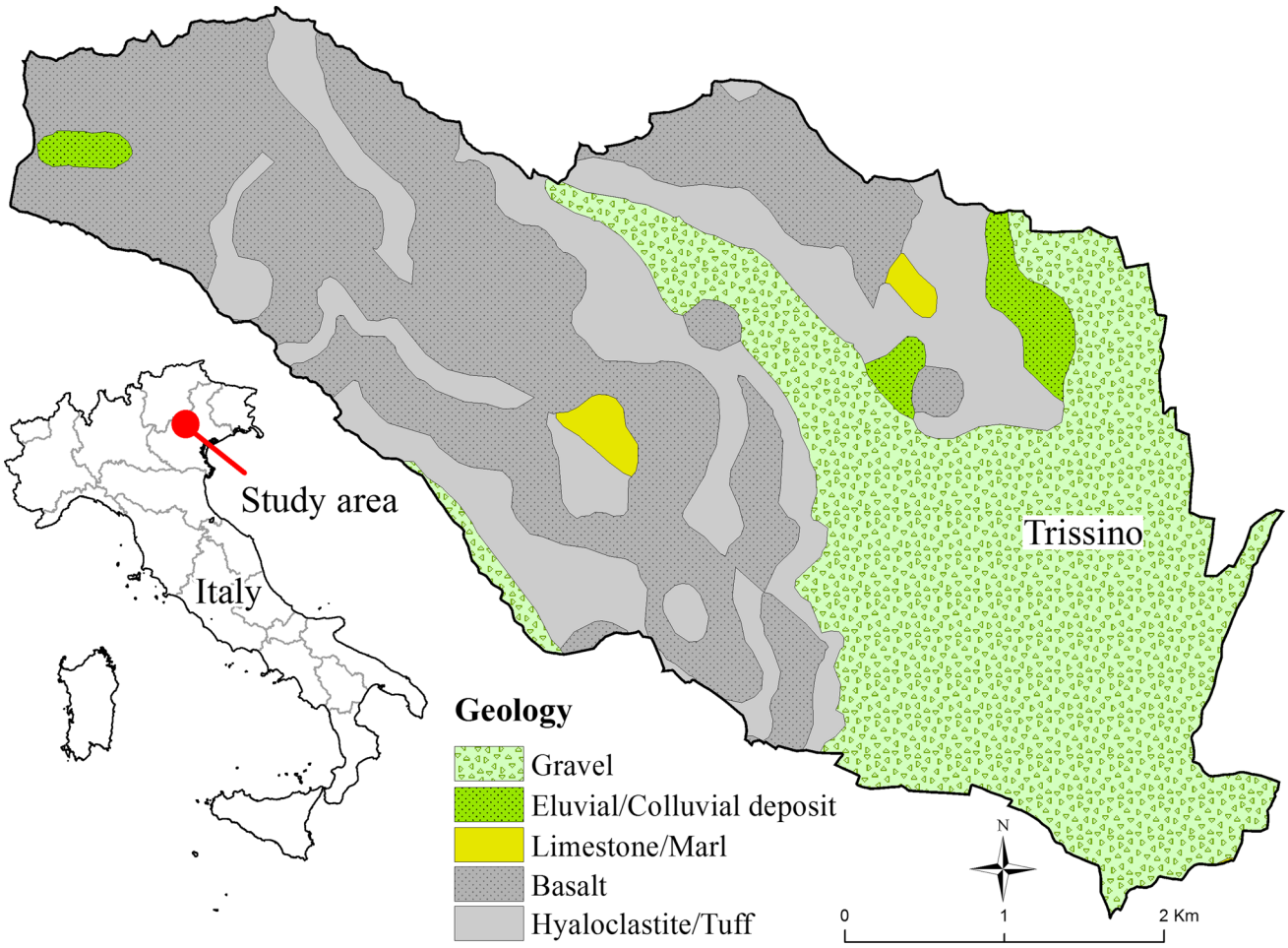

Fig. 1 Location of the study area and lithological map of the Municipality of Trissino (modified from ISPRA 2016)

the Vicenza Province received more than 500 warnings of instability phenomena (Floris et al. 2012) and in the Municipality of Trissino the activation of 12 landslides were documented (Fig. 2).

Mass movements generally involve the debris coverage or the terrain up to a maximum depth of 8 m and occur mainly between 250 and 400 m a.s.l. in the central section of the study area and between 450 and 600 m a.s.l. in the western section. Most of the landslides occur along the N-S and E direction, while only few along the W direction. The average velocity of movement that characterize the instabilities over large areas is generally below 10 mm/year, while smaller landslides generally occur suddenly with no warning signs. Even if these slope instabilities are not very large, they often occur near the urbanized areas damaging the buildings and the infrastructure, in particular the road network, and causing significant disruptions of daily life and high economic losses (Fig. 3). Landslides prevention and control works such as the installation of drainage systems were carried in the most critical areas and are constantly monitored by the local authorities.

Methods

The Sentinel-1A data sets processed in this study consist of 46 scenes acquired from 12/2014 to 09/2016 with descending orbit number 95 and 42 scene acquired from 03/2015 to 09/2016 with ascending orbit number 117. The ground resolution achievable with the Sentinel-1A C-band sensor is around 20 m $\times$ 20 m applying a multi-look factor of 5 in range and 1 in azimuth. In order to reduce processing time, save disk space and, at the same time, to produce results that can be easily managed in a geographic information system (GIS) environment for the post-processing analyses, the acquisitions were resized to comprehend exclusively the study area (the Municipality of Trissino). The processing of the available images has been carried out through the PSI technique using the Precise Orbit Ephemerides (POE) orbit files (data available from ESA at: qc.sentinel1.eo.esa.int/aux_poeorb) to reduce the errors related to the satellite orbit inaccuracies. The main steps of the processing can be synthesized as follows: (1) first, the images are connected to create a network of

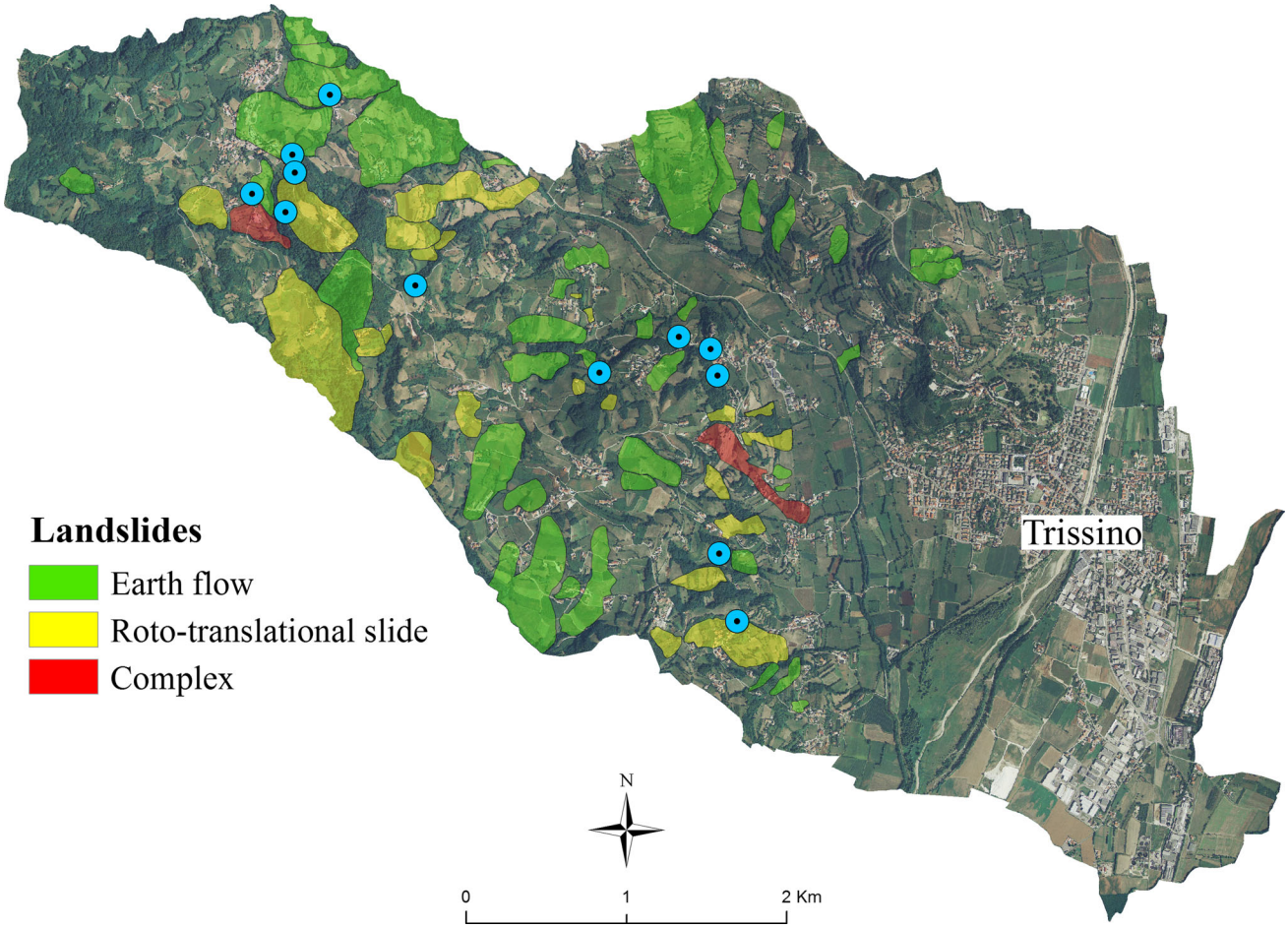

Fig. 2 Main landslides mapped within the study area. The *blue dots* are the location of the landslides occurred after the November 2010 exceptional rainfall event

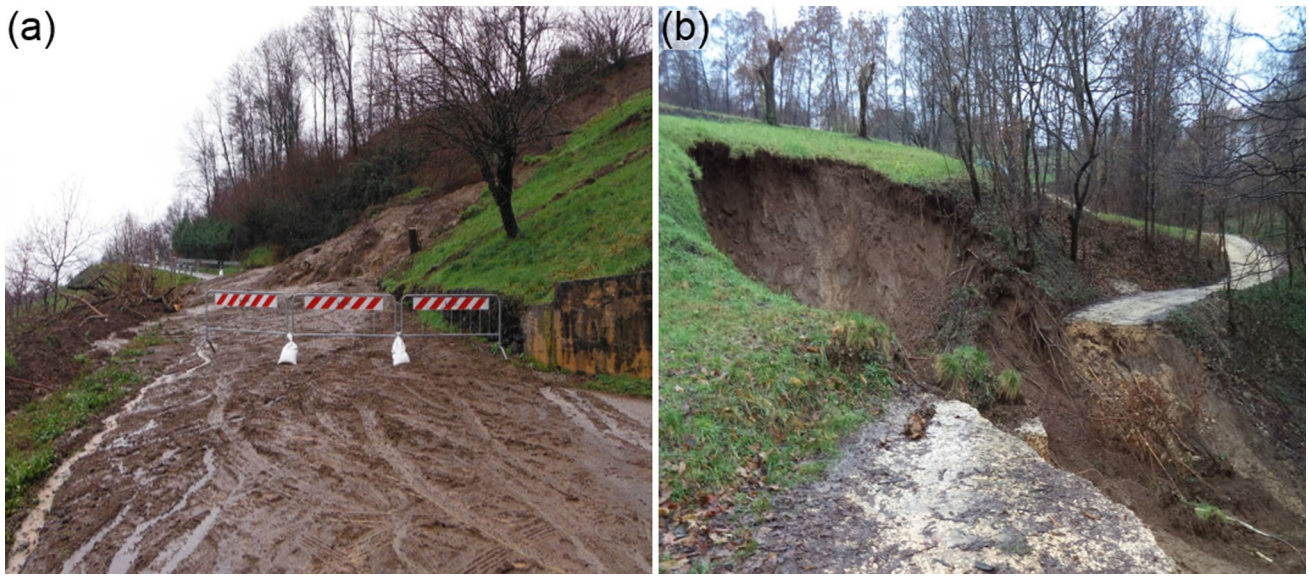

Fig. 3 Typical landslides occurring in the study area: **a** earth flow, **b** rotational slide/flow. In evidence the damage to the road network

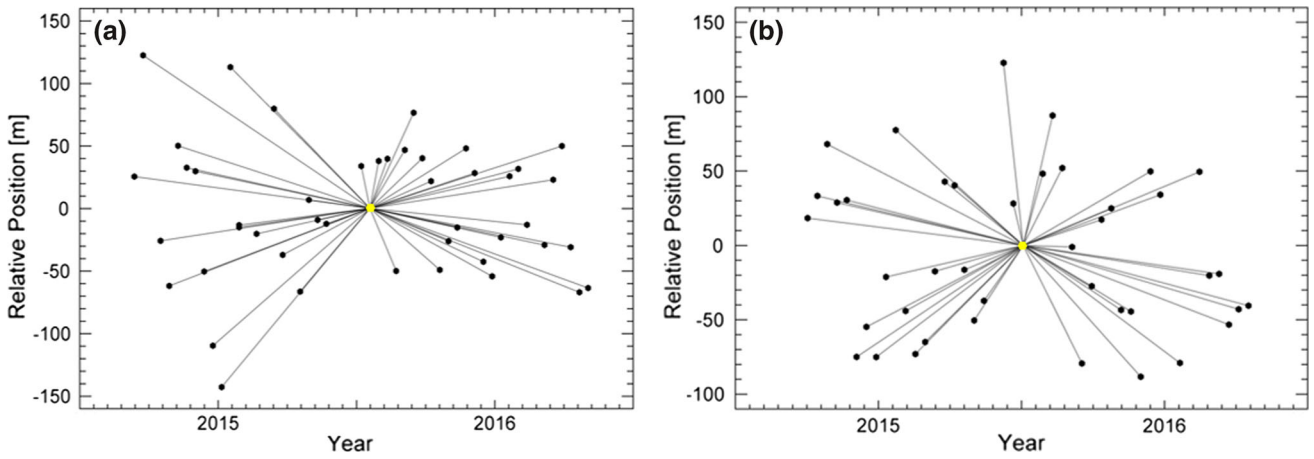

Fig. 4 Connection network between master (*yellow dot*) and slaves (*black dots*) images obtained from **a** 46 Sentinel-1A descending scenes and **b** 42 ascending scenes

master and slave pairs, using a single master image (Fig. 4); (2) the images are coregistered onto the master acquisition and the coherence image, and the interferograms and the related intensity images are generated. The interferograms are then flattened removing the constant phase (due to the acquisition geometry) and the topographic phase. For the latter, the February 2000 Shuttle Radar Topography Mission (SRTM) Digital Elevation Model (DEM) (Rabus et al. 2003; USGS 2006) with 30-m pixel size was used; (3) the phase-height pair-by-pair proportionality factors are estimated and removed from the flattened interferograms. The Persistent Scatterers (PS) candidates are then generated, and the displacement information (i.e. velocity) is estimated using the linear model:

$$\text{Disp} = V * (t - t0)$$

where Disp is the displacement at time t and V is the displacement velocity; (4) the spatial and temporal variations related to the atmospheric phase are estimated and subtracted from the interferograms in order to calculate the final displacements. The atmospheric correction is performed applying two filtering methods: the low-pass filtering, which accounts for the spatial distribution of the atmospheric variations and is implemented by using a square window of 1200 m; and the high-pass filter, which accounts for the temporal distribution of the atmospheric variations and uses a temporal window of 365 days. The PS candidates are then selected considering the coherence value, which identifies the level of backscattering that the targets on the ground maintain between two consecutive acquisitions. In this case, the coherence threshold was set to 0.80; (5) finally, all PS candidates are projected onto the adopted geographic coordinate system (GCS) WGS84. To improve results quality, the PS candidates can be further filtered in this step considering the amplitude dispersion index (μ/σ), which represents the ratio between the average SAR intensity (μ) and the standard deviation (σ). In this case, the adopted threshold was 3.2.

The obtained results were compared with the ERS-1/2 and ENVISAT PSI database available from the National Cartographic Portal (PCN) that were produced in the framework of the Special Remote Sensing Environment Plan, promoted by the Italian Ministry of Environment. Within the study area, the PSI results obtained from the following data sets were available: 79 descending ERS-1/2 images (04/1992–11/2000); 29 ascending ERS-1/2 images, (05/1992–06/2000); 34 descending ENVISAT images (01/2003–06/2010); and 34 ascending ENVISAT images, (12/2003–07/2010).

Results

The results obtained from the PSI analysis applied to the Sentinel-1A images are reported in terms of mean linear displacement velocity along the sensor line of sight (LOS) in Fig. 5. Positive values are colour coded in blue and refer to natural radar targets (the PS) moving towards the satellite, while negative values (in red) testify a displacement far from the satellite. Although the selected parameters were quite restrictive, 6203 PS candidates were generated with the descending data set, and 5855 with the ascending one. PSI analysis detects several areas affected by displacements, in particular in the north-west and the central sections of the Trissino Municipality. The range of the displacement velocities is generally low, with rates ranging from 2 to 7 mm/year, values that are in accordance

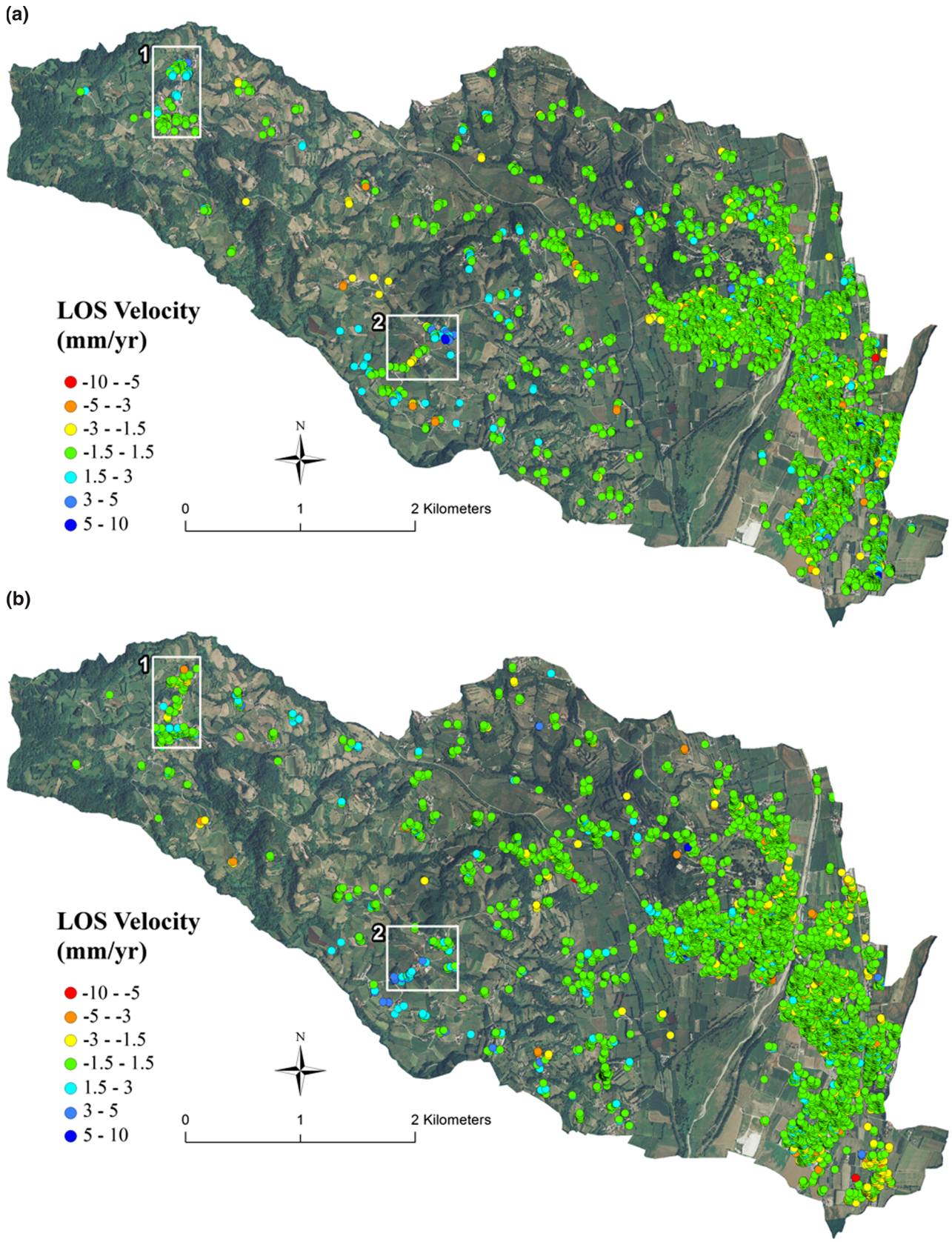

Fig. 5 LOS velocity maps obtained from descending **a** and ascending **b** Sentinel-1A data processing. *White boxes* indicate the specific unstable slopes reported in Figs. 6 and 7

Table 1 Comparison between the PS results obtained with Sentinel-1A, ENVISAT and ERS-1/2: image acquisition geometry; total number of PS; PS density; velocity standard deviation (σ); and percentage of moving PS

Satellite	Geometry	No. of PS	PS/Km^2	Velocity σ (mm/year)	Moving PS (Vel $\neq \pm$ 1.5 mm/year) (%)
Sentinel-1A	Descending	6203	283	0.54	12
ENVISAT	Descending	1204	54	0.69	6
ERS-1/2	Descending	1305	59	0.35	7
Sentinel-1A	Ascending	5855	267	0.69	18
ENVISAT	Ascending	992	45	0.44	2
ERS-1/2	Ascending	803	36	0.43	7

with the type of instabilities affecting the area. As it can be noticed from Fig. 5, most of the small urban agglomerates in the area are recording deformation patterns as consequence of the mobilization of the weak deposits triggered by intense rainfall. The use of images acquired in descending and ascending orbits permits a better characterization of the prevalent direction of the displacements allowing us to assess the components of plano-altimetric change. Furthermore, since the backscattering properties change with the satellite viewing geometry, the analysis of descending and ascending data sets increases the number and the spatial distribution of the PS within the area of interest.

The shorter revisit time of Sentinel-1A in respect to ERS-1/2 and ENVISAT (12 vs 35 days) allowed us to obtain a much higher PS density (Table 1) that positively reflects not only on the quantity but also on the quality of the measurements. Despite the restrictive processing thresholds adopted, the Sentinel-1A results are still affected by a moderate level of noise generated by an overall low signal-to-noise ratio, which is probably consequence of the short temporal extent of the available images stack (Hanssen 2005; Mahapatra et al. 2012). The presence of noise in the results can be noticed in Fig. 5 from the moving PS (red and blue dots) in the stable area (green dots) in the section occupied by the city of Trissino.

The comparison with the ERS-1/2 and ENVISAT PSI database shows a good agreement in the rates of movement and location of the landslides detected by each sensor (Figs. 6, 7). Figure 6 shows the displacements detected by the PSI analysis over area 1 of Fig. 5. As reported by the people living in this area, several houses have recently shown fissures and displacements of walls and sidewalks as sign of the terrain mobilization. Moreover, the complexity of the movements and the lack of geomorphological evidences make difficult to precisely map the extension of the landslide.

The opposite colour shift in the two data sets (blue for the descending acquisitions and orange for the ascending) witnesses a prevalent planimetric displacement towards E-SE of the buildings in the northern sectors; this direction of movement is in accordance with the one of the instability phenomenon. This result clearly shows the landslides distribution of activity (marked retrogressive) suggesting the necessity of reviewing its limits.

Figure 7 displays in detail another area affected by movement (area 2 of Fig. 5). In the SW sector, the direction of displacement towards W revealed by the ascending

Table 2 Number of PS falling in the mapped landslides

Satellite	Track	Landslides with PS $\geq$ 4	Flows with PS $\geq$ 4	Slides with PS $\geq$ 4	Landslides with 1 $\leq$ PS $<$ 4	Flows with 1 $\leq$ PS $<$ 4	Slides with 1 $\leq$ PS $<$ 4
Sent.-1A	Desc.	23 (36%)	17 (41%)	6 (26%)	13 (20%)	10 (24%)	3 (13%)
ENVISAT	Desc.	10 (16%)	8 (19%)	2 (9%)	29 (45%)	18 (44%)	11 (49%)
ERS-1/2	Desc.	17 (26%)	13 (32%)	4 (17%)	28 (44%)	18 (44%)	10 (43%)
Sent.-1A	Asc.	29 (45%)	19 (46%)	10 (43%)	12 (19%)	8 (19%)	4 (17%)
ENVISAT	Asc.	4 (6%)	2 (5%)	2 (9%)	26 (41%)	17 (41%)	9 (39%)
ERS-1/2	Asc.	8 (12%)	5 (12%)	3 (13%)	24 (37%)	16 (39%)	6 (26%)

In brackets the percentage respect to the total of the instability phenomena (41 flows and 23 slides)

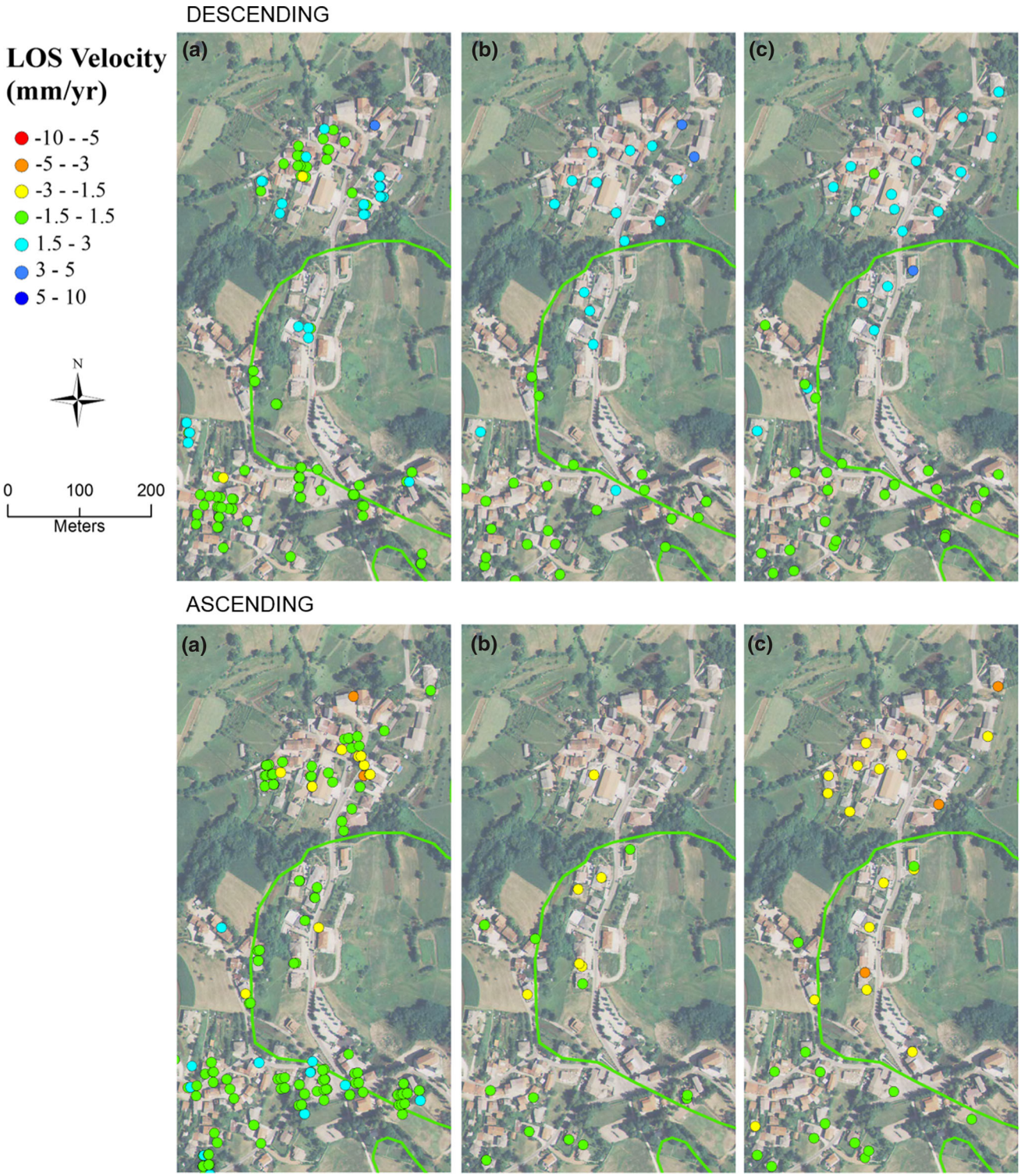

Fig. 6 LOS velocity maps of the north section of the study area (area 1 of Fig. 5) obtained from Sentinel-1A (**a**), ENVISAT (**b**) and ERS-1/2 (**c**) data sets. The *green lines* indicate the mapped landslide

orbit (positive values) is coherent with a retrogressive activity distribution of the instability. Furthermore, in the NE sector where no landslides were mapped before, it is clearly visible towards satellite movement of the area mainly in the E direction given by the positive values of the detected PS in descending orbit. In this case, of the 29 PS

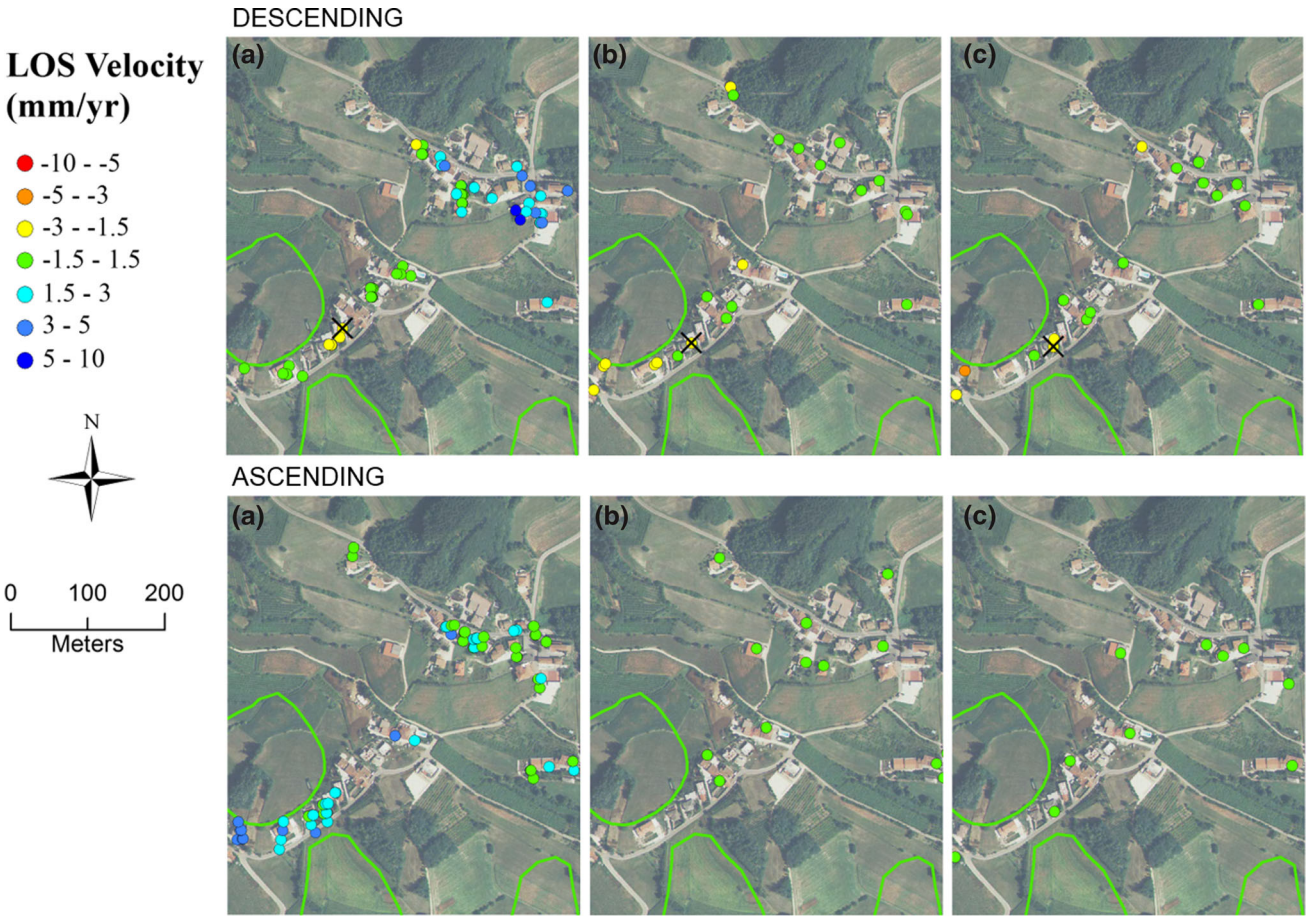

Fig. 7 LOS velocity maps of the middle section of the study area (area 2 of Fig. 5), obtained from Sentinel-1A (**a**), ENVISAT (**b**) and ERS-1/2 (**c**) data sets. The *green lines* indicate the mapped landslides. The displacement time series for the selected PS (*black cross*) are reported in Fig. 9

measured, 27 of them registered velocities in the range from 1.6 to 3.6 mm/year, while only two present higher velocities of 5.4 and 7.1 mm/year, which is the maximum value registered in the entire study area. Thus, also in this case, the landslides delimitation should be updated and more in depth remote and ground-based analyses are needed to characterize the landslide detected by the PSI analysis in the NE sector of Fig. 7.

Discussion

In order to assess the capabilities of the Sentinel-1A for landslide monitoring in such environment, the number of Sentinel-1A, ENVISAT and ERS-1/2 PS falling inside the mapped instabilities was calculated considering a buffer of 50 m around each landslide (Table 2). This buffer was adopted to compensate possible geocoding inaccuracies of the PS and imprecise delimitations of the instability phenomena. Assuming a threshold of PS $\geq$ 4 as the minimum to monitor the temporal evolution of mass movements (Cigna et al. 2013; Herrera et al. 2013; Notti et al. 2010), the results are quite encouraging: up to 45% of the landslides contain a number of PS above the threshold. More than the 50% of the landslides (64% in the case of ascending orbit) have at least one PS falling inside their limits. According to these results, the descending orbit is more suitable to detect flow type landslides than the slides, probably because of the morphological conditions (aspect) of the investigated territory. The results obtained with Sentinel-1A represent a great improvement in respect to the performance obtained with ERS-1/2 and ENVISAT and are comparable to the results achieved by some authors in other geomorphological contexts using medium- and high-resolution SAR data (Cigna et al. 2013; Herrera et al. 2013; Notti et al. 2010; Wasowski and Bovenga 2014).

The displacement trends of target reflectors selected in the stable area of the town of Trissino (Fig. 8) and in an unstable area (Fig. 9) are analysed in detail to further demonstrate the great improvement brought by the Sentinel-1A data for ground displacement monitoring purposes.

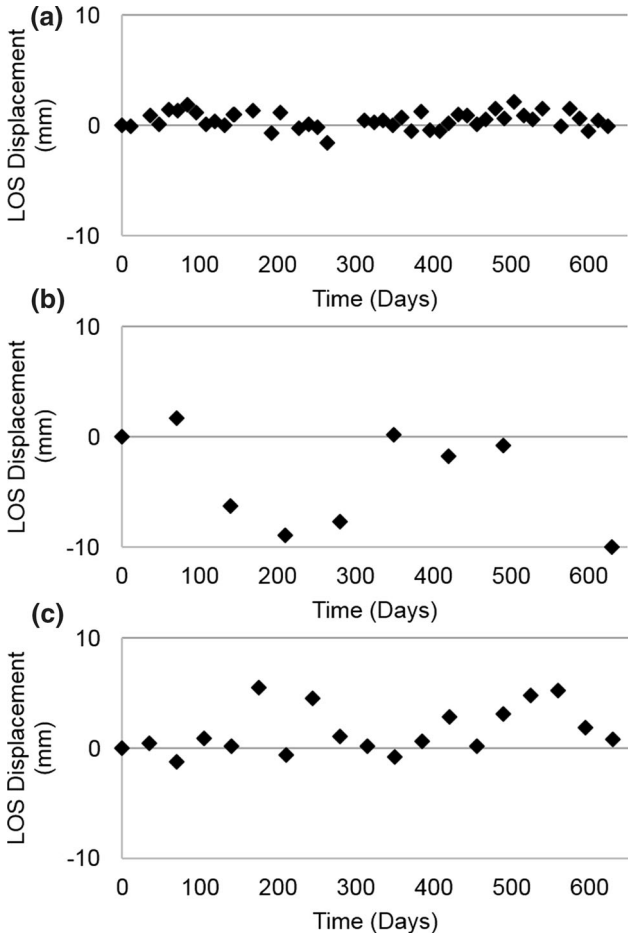

Fig. 8 Time series of a stable target selected in the town of Trissino: **a** Sentinel-1A, **b** ENVISAT and **c** ERS-1/2

In order to make the all the results comparable with the Sentinel-1A time series (624 days in total), a 630-day stretch was extracted from the original ENVISAT and ERS-1/2 time series: from January 2007 to October 2008 for ENVISAT, and from December 1996 until September 1998 for ERS-1/2. These stretches were chosen among those with the largest number of ENVISAT and ERS-1/2 acquisitions, covering the seasonal periods enclosed in the Sentinel-1A data sets (December 2014–September 2016). As it can be noticed from Fig. 8, the number of measurements plays and important role in the interpretation of the time series. If from one hand the 47 Sentinel-1A acquisitions clearly define the stability of the PS in the investigated period, on the other hand, the 10 ENVISAT measurements resulted in a very noisy scattered plot. Better results were obtained by the ERS-1/2 data set from which the stability of the area can be assumed even if some seasonal variations are evident. Assuming an expected value equal to 0 (no displacement), the standard deviations of the three measurements are 0.76, 5.03 and 2.16 mm, respectively, for the Sentinel-1A, ENVISAT and ERS-1/2 data sets.

Figure 9 shows that the displacement trend of a point located inside the landslide body of Fig. 7, chosen as example, is evident with Sentinel-1A measurements (besides a clear unwrapping error in the fourth interferogram), while with ENVISAT and ERS-1/2 the noise is predominant, making difficult the correct interpretation of the movement trend. In the latter case, only by analysing a longer time series, as reported in Fig. 9 d and e, the deformation trends can be correctly inferred.

The results obtained in this study depicts the great improvements brought by Sentinel-1 in the exploitation of A-DInSAR techniques for the detection and monitoring of slope instabilities. The combination of C-band and short revisit time of 12 days greatly reduced the temporal decorrelation allowing us to obtain point density five times higher than the older C-band satellites (i.e. ERS-1/2 and ENVISAT) previously used to monitor the same area. This permitted the identification of a large number of moving targets corresponding to new or recently re-activated landslides. From the analysis of the time series, it is possible to extract information about quiescence periods or intermittent activations that is crucial to better understand the landslide behaviour and its relationship with the triggering factors. This information is lost using ERS-1/2 and ENVISAT data because of the 35-day time span between the acquisitions.

Similar results and considerations were also described by other authors that successfully exploited Sentinel-1A SAR images for landslides mapping in different study areas (e.g. Barra et al. 2016; Crosetto et al. 2016). Despite the limitations of the A-DInSAR techniques in mountain territories (mainly given by the slope orientation and the vegetation coverage), this study demonstrates that Sentinel-1 can be a reliable and cost-effective tool for the monitoring of the territory on a regular basis which informative output can be of huge benefit in particular in the framework of landslides risk assessment and mitigation. This approach can be also used by the authorities to update regional and national landslides inventory maps (Lazecky et al. 2016) rapidly and at minimum costs. However, SAR data must always be integrated with case-specific ground-based analysis and cannot be used as the only source of information for the precise characterization of slope instabilities.

Conclusions

In this work, we tested the potential of the Sentinel-1A satellite SAR data in the monitoring of a densely vegetated area in the northern Italy affected by small to medium size landslides. To this end, 46 descending and 42 ascending Sentinel-1A images acquired, respectively,

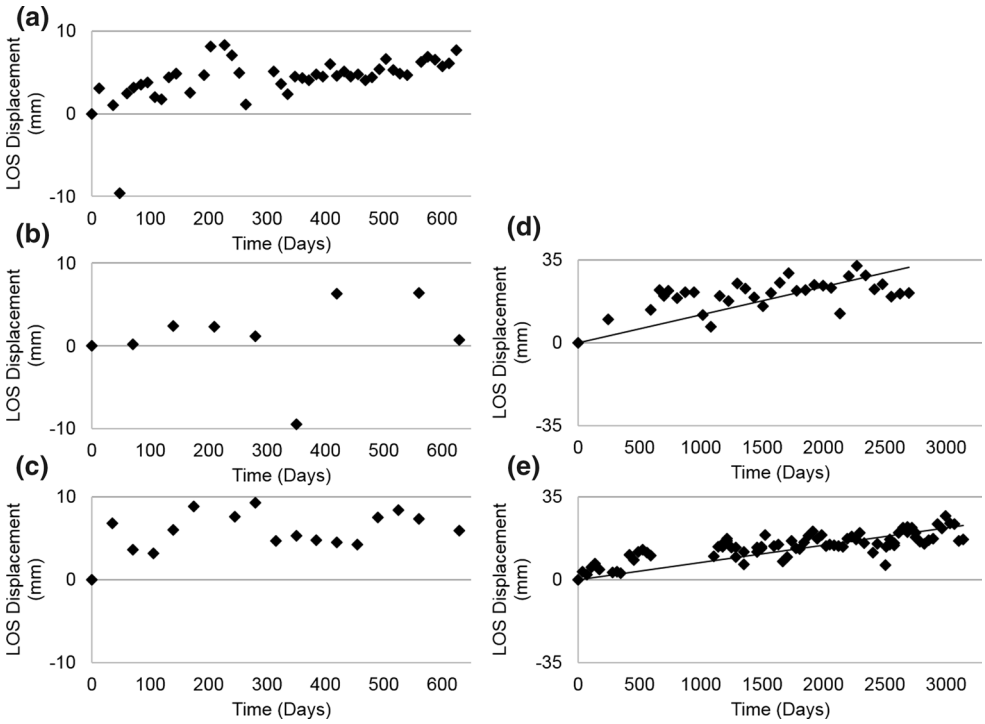

Fig. 9 Time series of moving targets selected over a landslide body obtained with Sentinel-A (**a**), ENVISAT (**b**), ERS-1/2 (**c**); **d**, **e** show the full-length time series, respectively, of ENVISAT and ERS-1/2

from 12/2014 to 09/2016 and from 03/2015 to 09/2016 have been processed using the PSI technique. First insights on the potential of Sentinel-1 mission to detect landslides are reported in previous works (e.g. Barra et al. 2016; Crosetto et al. 2016; Lazecky et al. 2016); nevertheless, in this study the results were compared, for the first time with those of the ERS-1/2 (1992–2000) and ENVISAT (2003–2010) PSI archive available from the National Cartographic Portal of the Ministry of Environment. Sentinel-1A results show that among the 64 mapped landslides, the 45% have more than four measured PS falling inside their limits, and the 64% have at least 1 PS. The movement rates are generally low, reaching at maximum 7 mm/year. The obtained results show the great potential of the Sentinel-1A data in the continuous monitoring of landslide-prone territories not only limiting the activity at the regional scale, but also focusing on local scale phenomena. The high number of PS obtained with Sentinel-1A and the high temporal sampling rate of the measurements can help to better characterize the movements in the area, to delineate the extent of several landslides, and to detect new instability phenomena. Such results represent a great improvement in the detection and monitoring of landslides in respect to the previous ERS-1/2 and ENVISAT C-band satellites, and they can be comparable to the results achievable by using high-resolution X-band SAR data. Even if there are only less than 2 years of acquisitions available, the measurements carried out with Sentinel-1A can correctly assess the rate of deformation of natural target reflectors. These results, as demonstrated, are hardly achievable in such a short period from previous satellite missions (e.g. ERS-1/2 and ENVISAT). The availability of new images and the extension of the temporal coverage will increase the overall quality of the achievable results. Moreover, the twin Sentinel-1B satellite launched in April 2016 will supply the scientific community with an additional set of SAR images that will permit, combining the data from both satellites, to lower the image frequency to 6 days, with great benefits in terms of detection capabilities and quality of the results. Sentinel-1 exploitation can provide very useful information about the spatial and temporal evolution of landslides. A continuous monitoring activity is crucial especially in critical areas to keep track of the landslides movement over time and to assess abrupt changes in the deformation rates. However, since the PS are limited to high backscattering objects (namely, the buildings), it is not possible to rely only on A-DInSAR techniques to precisely delineate the extension of an active landslide, which limits may interest vegetated areas where no measure points are available. For this reason, geological surveys are always necessary in order to check the presence of geomorphological evidences that are sign of active movements.

Acknowledgements ERS-1/2 and ENVISAT data sets were processed by Tele-Rilevamento Europa (TRE S.r.l.) in the framework of the Special Remote Sensing Environment Plan, promoted by the Italian Ministry of Environment. These results are available from the National Cartographic Portal (PCN) at www.pcn.minambiente.it. Sentinel-1A images are freely available from the European Space Agency (ESA) Sentinel-1 Open Access Hub (https://scihub.copernicus.eu). The authors would like to thank the anonymous reviewers for their detailed comments and suggestions for the manuscript.

References

Barra A, Monserrat O, Mazzanti P, Esposito C, Crosetto M, Scarascia Mugnozza G (2016) First insights on the potential of Sentinel-1 for landslides detection. Geomat Nat Hazard Risk 7(6):1874–1883. doi:10.1080/19475705.2016.1171258

Beccaro L, Fornaciari E, Mietto P, Preto N (2001) Analisi di facies e ricostruzione paleoambientale della rampa dei "Calcari nummulitici" (Eocene; Monti Lessini orientali–Vicenza): dati preliminari. Studi Trentini di Scienze Naturali - Acta Geologica 76(1999):3–16

Biggs J, Anthony EY, Ebinger CJ (2009) Multiple inflation and deflation events at Kenyan volcanoes, East Africa Rift. Geology 37(11):979–982. doi:10.1130/G30133A.1

Cascini L, Fornaro G, Peduto D (2009) Analysis at medium scale of low-resolution DInSAR data in slow-moving landslide affected areas. ISPRS J Photogramm Remote Sens 64(6):598–611. doi:10.1016/j.isprsjprs.2009.05.003

Cascini L, Fornaro G, Peduto D (2010) Andvanced low- and full-resolution DInSAR map generation for slow-moving landslide analysis at differential scales. Eng Geol 112(1–4):29–42. doi:10.1016/j.enggeo.2010.01.003

Casu F, Manconi A, Pepe A, Lanari R (2011) Deformation time-series generation in areas characterized by large displacement dynamics: the SAR amplitude pixel-offset SBAS technique. IEEE T Geosci Remote 49(7):2752–2763

Chaabane F, Tupin F, Maitre H (2005) An empirical model for interferometric coherence. In: Proceedings of SPIE–the international society for optical engineering 5980, art. no. 59800E. doi:10.1117/12.627341

Cigna F, Bianchini S, Casagli N (2013) How to assess landslide activity and intensity with Persistent Scatterer Interferometry (PSI): the PSI-based matrix approach. Landslides 10(3):267–283. doi:10.1007/s10346-012-0335-7

Colesanti C, Wasowsky J (2006) Investigating landslides with space-borne Synthetic Aperture Radar (SAR) interferometry. Eng Geol 88(3–4):173–199. doi:10.1016/j.enggeo.2006.09.013

Colombo A, Mallen L, Pispico R, Giannico C, Bianchi M, Savio G (2006) Mappatura regionale delle aree monitorabili mediante l'uso della tecnica PS. In: Proceedings of 10th national conference ASITA, November 14–17, 2006, Bolzano, Italy (ISBN/ISSN: 88-900943-0-3-2006)

Crosetto M, Monserrat O, Devanthérya N, Cuevas-González M, Barra A, Crippa B (2016) Persistent Scatterer Interferometry using Sentinel-1 data. In: ISPRS-international archives of the photogrammetry, remote sensing and spatial information sciences pp 835–839. XXIII ISPRS Congress, 12–19 July 2016, Prague, Czech Republic

Cruden DM, Varnes DJ (1996) Landslide types and processes. In: Special Report 247–landslides: investigation and mitigation. Transportation Research Board, Washington, DC

Ferretti A, Prati C, Rocca F (2001) Permanent scatterers in SAR interferometry. IEEE Trans Geosci Remote 39(1):8–20

Floris M, D'Alpaos A, De Agostini A, Stevan G, Tessari G, Genevois R (2012) A process-based model for the definition of hydrological alert systems in landslide risk mitigation. Nat Hazards Earth Syst Sci 12:3343–3357. doi:10.5194/nhess-12-3343-2012

Garavello AM, Ungaro S (1996) Biostratigrafia del Paleocene ed Eocene Inferiore dei M. Lessini. Sezione stratigrafica di Gazzo (Verona). Annali dell'Università di Ferrara, sezione Scienze della Terra 7:23–34

Hanssen R (2005) Satellite radar interferometry for deformation monitoring: a priori assessment of feasibility and accuracy. Int J Appl Earth Obs Geoinf 6:253–260. doi:10.1016/j.jag.2004.10.004

Herrera G, Gutiérrez F, García-Davalillo JC, Guerrero J, Notti D, Galve JP, Fernández-Merodo JA, Cooksley G (2013) Multi-sensor advanced DInSAR monitoring of very slow landslides: the Tena Valley case study (Central Spanish Pyrenees). Remote Sens Environ 128:31–43. doi:10.1016/j.rse.2012.09.020

ISPRA (Italian National Institute for Environmental Protection and Research) (2016) The Geological Survey of Italy mapping. Mem. Descr. Carta Geol. d'It. 100:73–92

Lazecky M, Canaslan Comut F, Nikolaeva E, Bakon M, Papco J, Ruiz-Armenteros AM, Qin Y, de Sousa JJM, Ondrejka P (2016) Potential of Sentinel-1A for nation-wide routine updates of active Landslide maps. ISPRS Arch XLI-B7:775–781. doi:10.5194/isprsarchives-XLI-B7-775-2016

Mahapatra P, Samiei-Esfahany S, Hansen R (2012) Towards repeatability, reliability and robustness in time-series InSAR. In: Proceedings of fringe 2011 workshop, September 19–23, 2011, Frascati, Italy. ESA Special Publication, SP-697 (January 2012, CD. ISBN 978-92-9092-261-2, ISSN 1609-042X)

Manconi A, Casu F, Ardizzone F, Bonano M, Cardinali M, De Luca C, Gueguen E, Marchesini I, Parise M, Vennari C, Lanari R, Guzzeti F (2014) Brief communication: rapid mapping of landslide events: the 3 December 2013 Montescaglioso landslide, Italy. Nat Hazard Earth Syst Sci 14:1835–1841. doi:10.5194/nhess-14-1835-2014

McCann T (2008) The geology of central Europe. Geological Society of London, London

Michel R, Avouac JP (1999) Measuring ground displacement from SAR amplitude images: application to the Landers earthquake. Geophys Res Lett 26(7):875–878. doi:10.1029/1999GL900138

Notti D, Davalillo JC, Herrera G, Mora O (2010) Assessment of the performance of X-band satellite radar data for landslide mapping and monitoring: upper Tena valley case study. Nat Hazards Earth Syst Sci 10:1865–1875. doi:10.5194/nhess-10-1865-2010

Plank S, Singer J, Thuro K (2012) Estimation of the persistent scatterer density using optical remote sensing data and land cover data. In: Proceedings of fringe 2011 workshop, September 19–23, 2011, Frascati, Italy. ESA Special Publication, SP-697, January 2012, CD. ISBN 978-92-9092-261-2, ISSN 1609-042X

Plank S, Singer J, Thuro K (2013) Assessment of number and distribution of persistent scatterers prior to radar acquisition using open access land cover and topographical data. ISPRS J Photogramm Remote Sens 85:132–147. doi:10.1016/j.isprsjprs.2013.09.001

Rabus B, Eineder M, Roth A, Bamler R (2003) The shuttle radar topography mission–a new class of digital elevation models acquired by spaceborne radar. ISPRS J Photogramm Remote Sens 57:241–262

Singleton A, Li Z, Hoey T, Muller JP (2014) Evaluation sub-pixel offset techniques as an alternative to D-InSAR for monitoring episodic landslide movements in vegetated terrain. Remote Sens Environ 147:133–144. doi:10.1016/j.rse.2014.03.003

Tomás R, Romero R, Mulas J, Marturià JJ, Mallorquí JJ, Lopez-Sanchez JM, Herrera G, Gutiérrez F, González PJ, Fernández J, Duque S, Concha-Dimas A, Cocksley G, Castañeda C, Carrasco

D, Blanco P (2014) Radar interferometry techniques for the study of ground subsidence phenomena: a re-view of practical issues through cases in Spain. Environ Earth Sci 71(1):163–181. doi:10.1007/s12665-013-2422-z

Tosi L, Da Lio C, Strozzi T, Teatini P (2016) Combining L- and X-band SAR interferometry to assess ground displacements in heterogeneous coastal environments: the Po River Delta and Venice Lagoon, Italy. Remote Sens 8:308. doi:10.3390/rs8040308

USGS (2006) Shuttle Radar Topography Mission, 1 arc second scene. Global Land Cover Facility, University of Maryland, College Park, Maryland, February 2000

Wasowski J, Bovenga F (2014) Investigating landslides and unstable slopes with satellite Multi Temporal Interferometry: current issues and future perspectives. Eng Geol 174:103–138. doi:10.1016/j.enggeo.2014.03.003

Wasowski J, Bovenga F, Nitti DO, Nutricato R (2012) Investigating landslides with Persistent Scatterers Interferometry (PSI): current issues and challenges. In: Eberhardt E, Froese C, Turner AK, Leroueil S (eds) Proceedings of the 11th international and 2nd North American Symposium on Landslides, Banff (Canada), 3–8 June, 2012. Landslides and Engineered Slopes, vol 2. CRC Press/Balkema, Leiden, The Netherlands, pp 1295–1301

Wasowski J, Bovenga F, Nutricato R, Nitti DO, Chiaradia MT, Refice A, Pasquariello G (2016) Exploring the potential of Sentinel-1 data for regional scale slope instability detection using multi-temporal interferometry, vol 18. EGU General Assembly 2016, Vienna, Austria, 17–22 April 2016, p 12505

Wright TJ, Ebinger C, Biggs J, Ayele A, Yirgu G, Keir D, Stork A (2006) Magma-manteined tirf segmentation at continental rupture in the 2005 Afar dyking episode. Nature. doi:10.1038/nature04978